



V #	Date	Type of revision	Author
0	24/02/2020	Published version	WP3

**Deliverable Contributors**

---

Authors

Partner	Name
KEP	Christophe Mathonat
KEP	Laurent Passelegue
KEP IC	Bruno Marmoux
KEP IC	Andrea Francescon
KEP IC	Lotfi Eddaoudi
KEP IC	Xavier Mettan
KEP IC	Charles Thoumyre
WUT	Wojciech Kubinski

Contributors

Partner	Name
KEP Nuclear	Christophe Mathonat
KEP	Laurent Passelegue
KEP IC	Bruno Marmoux
KEP IC	Andrea Francescon
KEP IC	Lotfi Eddaoudi
KEP IC	Xavier Mettan
KEP IC	Charles Thoumyre

Internal Reviewers

Partner	Name
Andra	Denise Ricard



## Table of Contents

<b>1</b>	<b>GLOSSARY</b> .....	<b>6</b>
<b>2</b>	<b>EXECUTIVE SUMMARY</b> .....	<b>7</b>
2.1	EXECUTIVE FACTSHEET .....	7
2.2	EXECUTIVE SUMMARY .....	7
<b>3</b>	<b>INTRODUCTION</b> .....	<b>8</b>
<b>4</b>	<b>CALORIMETER DESCRIPTION</b> .....	<b>9</b>
4.1	SPECIFICATIONS .....	9
4.2	OVERALL DIMENSIONS .....	10
4.3	PRINCIPLE .....	12
4.4	SOFTWARE .....	12
4.5	CALORIMETER OVERVIEW .....	13
<b>5</b>	<b>CALIBRATION PROCEDURE, TEST MEASUREMENTS AND EVALUATION OF UNCERTAINTIES ON THE LARGE VOLUME CALORIMETER (LVC) CHANCE</b> .....	<b>15</b>
5.1	INTRODUCTION.....	15
5.1.1	<i>Non-destructive measurement of the mass of radioactive assay</i> .....	15
5.1.2	<i>Principle of operation</i> .....	15
5.2	SOURCES OF UNCERTAINTIES .....	16
5.2.1	<i>Heat power</i> .....	16
5.2.2	<i>Uncertainties on the heat flow</i> .....	17
5.2.3	<i>Uncertainties on the sensitivity <math>S</math></i> .....	18
5.2.4	<i>Uncertainties on derived quantities</i> .....	20
5.3	ANALYSIS OF EXPERIMENTAL DATA .....	20
5.3.1	<i>Calibration of the LVC CHANCE</i> .....	20
5.3.2	<i>Determination of sensitivity</i> .....	22
5.4	SUMMARY .....	24
5.5	CONCLUSIONS .....	26
	<b>APPENDIX A – ERROR-PROPAGATION RULES</b> .....	<b>27</b>
	<b>APPENDIX B – THERMAL CONCEPTION OF THE CALORIMETER</b> .....	<b>28</b>
<b>6</b>	<b>BIBLIOGRAPHY</b> .....	<b>29</b>



## Table of Tables

TABLE 1 - SPECIFICATIONS .....9  
 TABLE 2- RESULTS OF PERFORMED MEASUREMENTS. VALUES AND UNCERTAINTIES WERE CALCULATED USING  
 FORMULAS FROM CHAPTER 5.....21  
 TABLE 3 - SENSITIVITY CALCULATED FOR EACH CALIBRATION POINT.....22  
 TABLE 4 - LINEAR REGRESSION, RESULTS. ....23  
 TABLE 5 - TLS METHOD, RESULTS. ....23  
 TABLE 6 - WEIGHTED LINEAR REGRESSION, RESULTS. ....24  
 TABLE 7 - SUMMARY OF THE RESULTS.....24  
 TABLE 8 - RELATIVE FIT ERRORS OF CONSIDERED METHODS, SUMMARY. ....25



**Tables of Figures**

FIGURE 1 - EXECUTIVE FACTSHEET ..... 7  
 FIGURE 2 - CHANCE LVC FRONT VIEW ..... 10  
 FIGURE 3 - CHANCE LVC SIDE VIEW ..... 11  
 FIGURE 4 - CHANCE LVC BOTTOM VIEW ..... 11  
 FIGURE 5 - CAD VIEW AND REAL PICTURE OF THE LVC CHANCE CALORIMETER..... 12  
 FIGURE 6 - LVC CHANCE IN KEP NUCLEAR FACILITY ..... 13  
 FIGURE 7 – LVC CHANCE INSTALLED IN CEA CADARACHE ..... 14  
 FIGURE 8 - THERMAL TRANSFERS BETWEEN THE NUCLEAR ASSAY AND THE LEFT, RIGHT AND CENTRE PARTS OF THE CALORIMETER (NOT TO SCALE). EACH ARROW DEPICTS HEAT FLUXES INSIDE THE CALORIMETER. THESE FLUXES GENERATE INDEPENDENT VOLTAGE SIGNALS  $V_i$  MEASURED BY AN ASSEMBLY OF PELTIER ELEMENTS. ALL THESE CONTRIBUTIONS ARE SUMMED ACCORDING TO EQ. (3) TO GIVE THE SIGNAL VOLTAGE  $V_s$  ..... 16  
 FIGURE 9 - EXAMPLE OF A DIFFERENTIAL VOLTAGE SIGNAL ( $V_s(t)$ ) SUBJECTED TO FLUCTUATIONS AROUND ITS AVERAGE VALUE OF  $V_s = 98.49 \mu V$  OVER TIME. THE STANDARD DEVIATION FOR  $N$  SAMPLES IS  $\sigma_s = \frac{1}{N} \sqrt{\sum (V_{stj} - V_s)^2}$  ..... 17  
 FIGURE 10 - SCHEME OF CALIBRATION PROCEDURE FOR 50MW JOULE EFFECT. .... 18  
 FIGURE 11 - TIME CHART OF THE HEAT FLOW RECORDED BY CALISTO (SOFTWARE) DURING TWO DUTY CYCLES OF A “JOULE-EFFECT” MEASUREMENT AT 250 MW OF INJECTED POWER. THE BLUE LINE IS THE HEAT FLOW SIGNAL (RIGHT AXIS) AND THE BLACK LINE IS THE JOULE POWER (LEFT AXIS). .... 21  
 FIGURE 12 - TLS FIT METHOD ..... 23  
 FIGURE 13 - RELATIVE FIT ERRORS OF CONSIDERED METHODS, SUMMARY..... 25  
 FIGURE 14 - PRINCIPLE OF CHANCE CALORIMETER OPERATION..... 28



# 1 Glossary

tion / Acronym	Description/meaning
CHANCE	Characterisation of conditioned nuclear waste for its Safe Disposal in Europe
KEPIC	KEP Innovation Center
LVC	Large Volume Calorimeter
RN	Radionuclide



## 2 Executive Summary

### 2.1 Executive Factsheet

Who should read this deliverable? Who are the stakeholders concerned by this deliverable?	Why should s/he read this deliverable? What will s/he learn from this deliverable?	Which part of the content is most relevant for him / her?
CEA ; SCK•CEN, WP3 partners	This document is presenting the calorimeter which will be used by CEA and SCK•CEN for Task 3.2.	Section 4
CHANCE partners other than WP3.	This section is useful for partners who are not involved in WP3 to get a broad picture of the calorimeter which will be used for characterizing radioactive waste.	Sections 4 & 5

*Figure 1 - Executive Factsheet*

### 2.2 Executive Summary

In the frame of the Task 3.2 “Experimental investigation” ,a 200 liters calorimeter with lowered detection limit were developed, manufactured and tested by KEP Nuclear. This calorimeter will be used for measuring plutonium and other possibly hidden RN in realistic cases with 200 L drums. Measurements will be carry out with mock-up waste drums at CEA Cadarache and SCK•CEN. SCK-CEN will also perform measurements with a 200 L real unconditioned waste drum. This document presents the Large Volume Calorimeter developed so called “CHANCE LVC”. The performances of the calorimeter and the main technical characteristics are also described.



### 3 Introduction

---

Calorimetry is an experimental technique employed for the measurement of the thermal power generated by heat-producing substances (Mason, 1982). Calorimetry is exploited in a variety of fields including scientific research, medicine, industry, military research and biology.

Calorimetry has been successfully applied to the characterisation of nuclear materials that generates heat by alpha and beta particle decay in the range of thermal powers spanning from 1 mW to 135 W. It is mainly used for the assay of Plutonium and  $^{241}\text{Am}$  (either as a single isotope or mixed with Plutonium). According to (ASTM, 2016), the typical range of applicability for plutonium, corresponds to ~0.1 g to ~5 g depending on the isotopic composition. Calorimetry measurement was also successfully employed in the assessment of the amount of tritium in radioactive waste packages. Tritium assay has always been challenging as neither a destructive analysis on the waste nor a sampling of radioactive matter inside the package (strongly dependent on the physical state of tritium) can be envisaged (Galliez, et al., 2016). In addition, direct nuclear counting is also not viable because of the low energy of beta particles of tritium, which can be stopped by few microns of metal. Whereas calorimetry measures the heat produced by the interaction of beta particles with the matter, the  $^3\text{H}$  mass of the sample can be inferred by knowing the specific power of tritium (324 mW/g). The typical range of applicability of calorimetry measurement in the assay of tritium extends from ~1 mg to ~400 g.

In the frame of Task 3.2 (experimental investigation) of the CHANCE project, a new 200 litres calorimeter with lowered detection limit was developed, manufactured and tested by KEP Nuclear. This work was divided in four main phases:

- Development

The development was based on an existing calorimeter LVC1380 from KEP Technologies taking into account some new development in electronics, working mode and thermal insulation to lower the detection limit.

Development means radiological, thermal and mechanical modelling to optimize the performance of the instrument. It was followed up by some CAD (Computer Aided Design) work to design all the mechanical and insulation parts of the calorimeter and define the electrical and electronic components used to control and regulate the calorimeter in isothermal mode.

- Purchasing

Purchasing of all calorimeter parts was an important part of the task and took place during more than six months. Some parts (which are the cooling plates made up of copper tubes inserted in some aluminium plates) were received faulty from our provider and it delayed the beginning of the manufacturing of the calorimeter.

- Setup – test and calibration

Setup of the calorimeter in order to fix the parameters controlling the heating and temperatures of the calorimeter took more than three months. Then some tests and the calibration of the calorimeter was undertaken in order to define the sensitivity, detection limit and accuracy of the calorimeter.

- CE Compliance of the calorimeter.

Last part of the work was to check that the calorimeter was complying with the CE certification regarding protection of the user against electrical and mechanical risks. A user manual was written to comply with the CE certification and make possible the commissioning and use of the calorimeter.



## 4 Calorimeter description

The CHANCE LVC calorimeter is an instrument using one single cell and having a high sensitivity based on a unique principle.

The CHANCE LVC is using the differential calorimetric technic having the following characteristics:

- It is a NDA method (non-destructive assay).
- The maximum cylindrical sample volume is 260 litres.
- It is using three integrated electronic racks.
- It is using a Joule effect calibration (with a removable canister).
- It measures power on the range: 100 to 3 500 mW.
- The measurement accuracy is < 2,5 %, precision is < 2 %.
- It is using a so called CALISTO software interface used for thermal analysis and a special software module.
- It is easy to access to the sample thanks to the sample chamber accessible by opening two half shelves.

### 4.1 Specifications

*Table 1 - Specifications*

<b>Calorimeter type</b>	Heat flux isothermal differential measurement
<b>Cell number</b>	1
<b>Measurement cell volume (litres)</b>	260 (diameter 610 mm × height 890 mm)
<b>Measuring range (mW)</b>	100 – 3500
<b>Temperature working range (°C)</b>	25 – 30
<b>Room Temperature working conditions (°C)</b>	20 – 35
<b>Precision (%)</b>	2,5
<b>Accuracy (%)</b>	2
<b>Measuring time (days)</b>	> 10 days (with 200 litres cement drum)
<b>Cooling system</b>	Water bath
<b>Calibration system</b>	Electrical resistance (Joule effect system)
<b>External dimensions width / depth / height (mm)</b>	4540 x 2390 x 2325
<b>Weight (kg)</b>	12000



## 4.2 Overall dimensions

An overview in 2 dimensions of the calorimeter is given in the following figures.

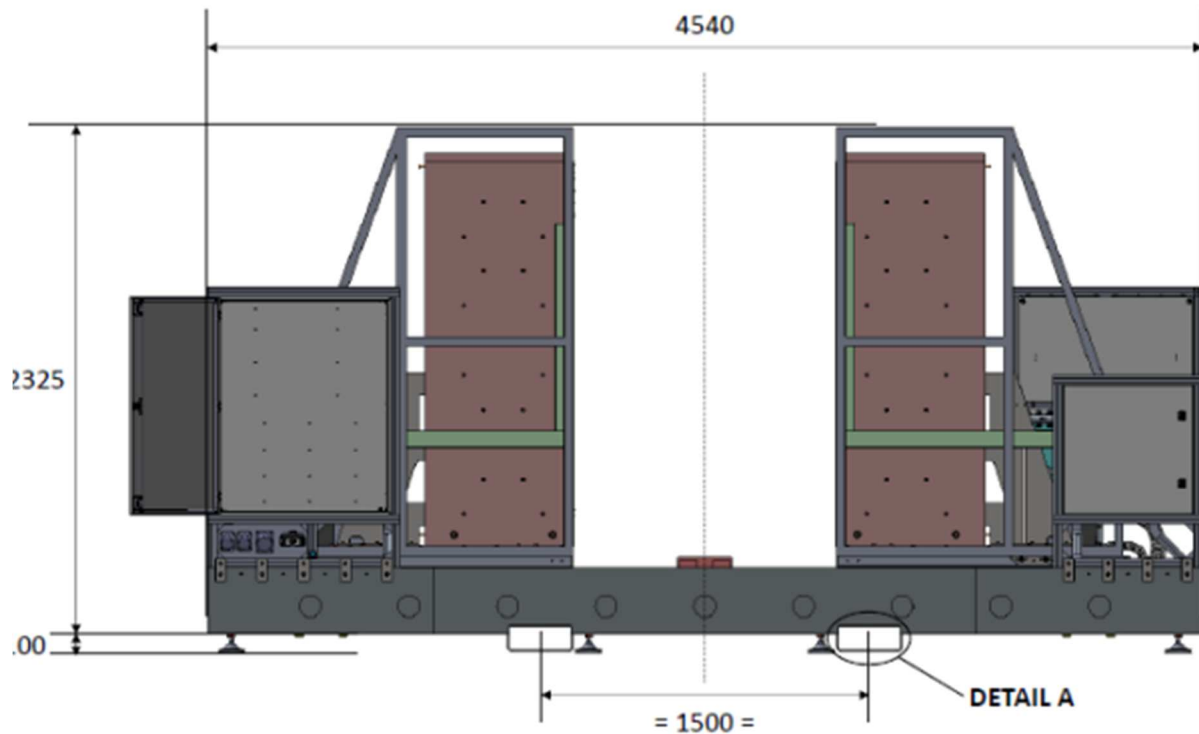


Figure 2 - CHANCE LVC front view

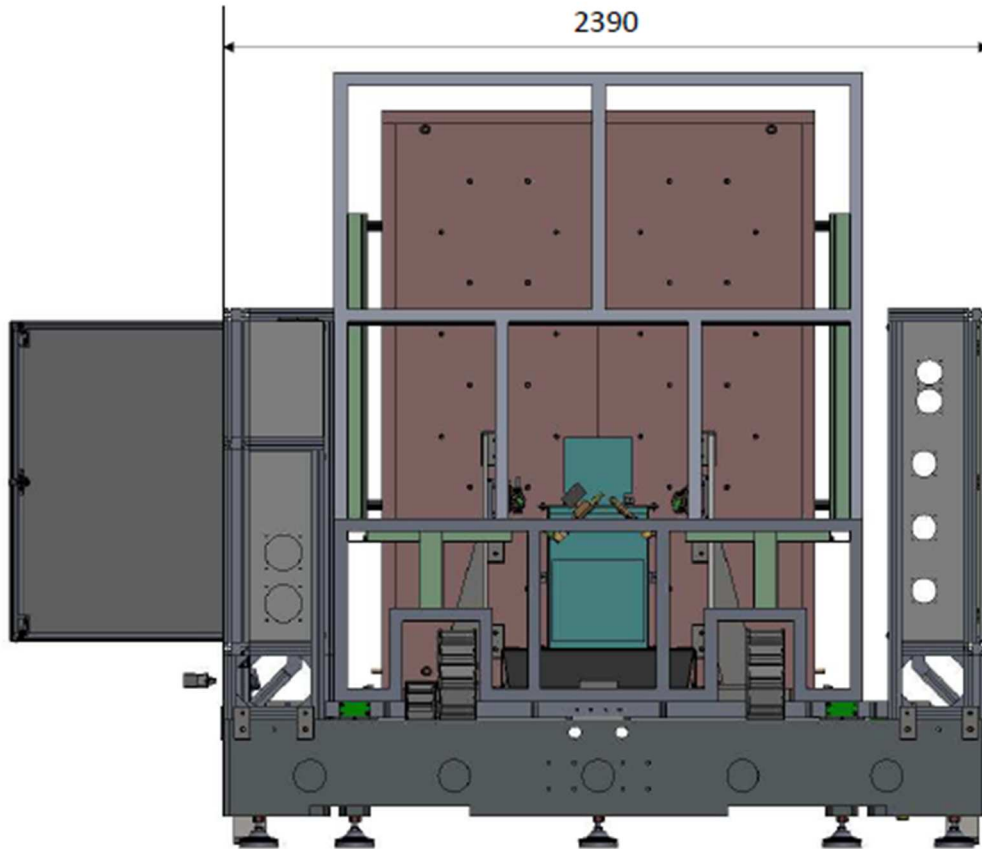


Figure 3 - CHANCE LVC side view

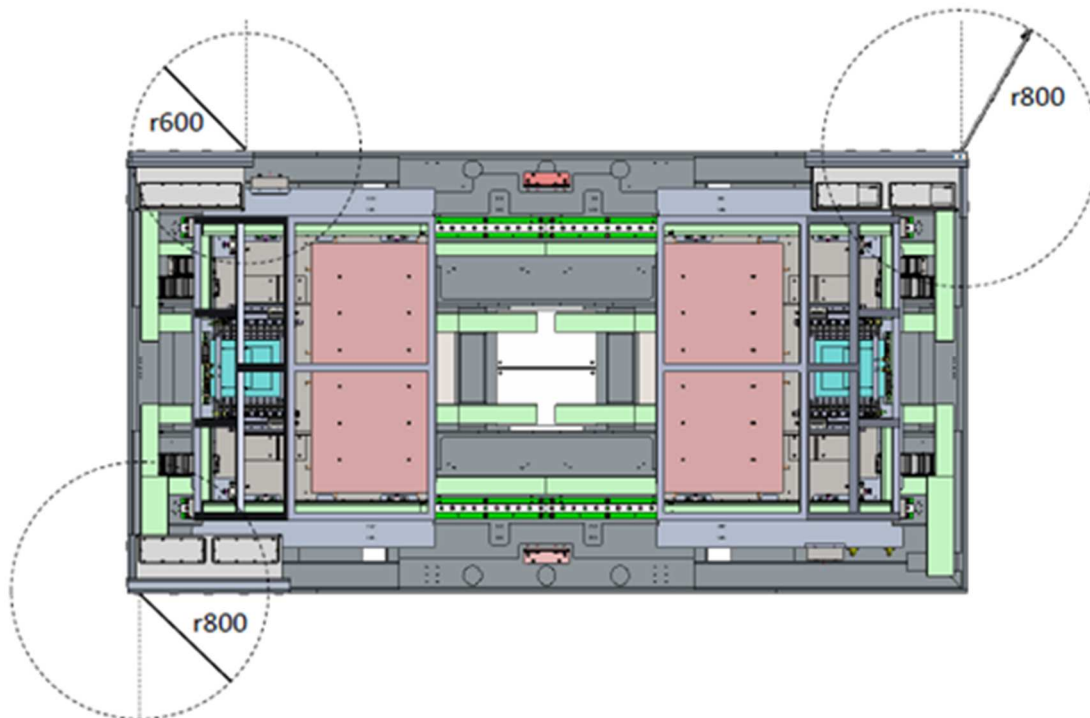
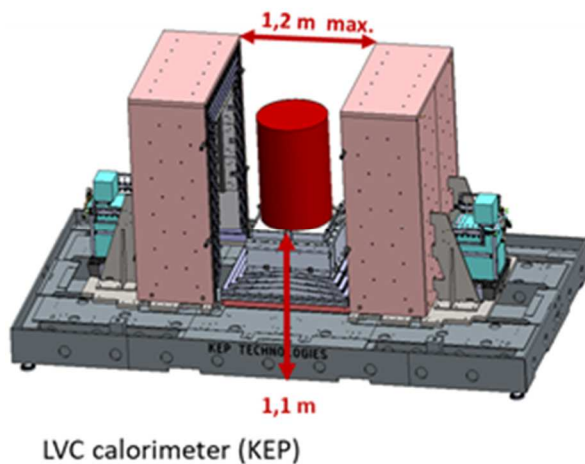


Figure 4 - CHANCE LVC bottom view

### 4.3 Principle

The CHANCE LVC is based on a calorimetric principle using some measuring and reference sensors surrounding the sample to be studied (drum) and collecting all the heat released by the sample.

The sensors are some Peltier elements generating a differential signal proportional to the deviation of the heat flux going through the measuring sensors from the one going through the reference sensors.



*Figure 5 - CAD view and real picture of the LVC CHANCE calorimeter*

The principle is more detailed in section 5

### 4.4 Software

The calorimeter is using the so called Calisto LVC software. It makes possible to setup the experimental conditions (working temperature and parameters to control the temperature regulation), to start the acquisition of an experiment and to process the results. It makes possible to calibrate the instrument by producing some well-known and precise wattages (Joule effect) inside a metallic canister placed in the calorimeter.

It is also using a dedicated software module developed for the CHANCE LVC making possible the acquisition of:

- All the parameters controlling the calorimeter (15 parameters giving some information about the heating of the different parts of the calorimeter);
- The temperature probes placed in the calorimeter (38 probes for left, right half shelves and centre block);
- Voltage produced by the Peltier elements in series (6 voltages corresponding to measuring and reference signals respectively for left, right and centre blocks);
- The resulting differential signal.

## 4.5 Calorimeter overview

A picture of the calorimeter in KEP Nuclear facility is presented below.



*Figure 6 - LVC CHANCE in KEP Nuclear Facility*

After testing the calorimeter in KEP Nuclear facility, it was send to CEA Cadarache at the end of November 2019



*Figure 7 – LVC CHANCE installed in CEA Cadarache*

## 5 Calibration procedure, test measurements and evaluation of uncertainties on the Large Volume Calorimeter (LVC) CHANCE

W. Kubiński, X. Mettan, C. Mathonat

### 5.1 Introduction

In this section we recall the calibration and measurement procedures on the Large Volume Calorimeter (LVC) CHANCE. We examine the influence of systematic and statistical uncertainty on the accuracy and precision of the calorimeters both theoretically and experimentally. In particular, the statistical treatment of calibration data is consolidated in order to provide the most reliable quantification of the activity of nuclear assays.

#### 5.1.1 Non-destructive measurement of the mass of radioactive assay

The thermal power generated by a sample of mass  $m$  is:

$$W_{\text{item}} = P_{\text{eff}} \cdot m, \quad (1)$$

where  $P_{\text{eff}}$  is the **specific power** of the sample. The specific power is determined by additional non-destructive methods (e.g. High Resolution Gamma Spectrometry), providing the percentage of a given isotope  $R_i$  with known specific power  $P_i$ , with  $P_{\text{eff}} = \sum_i R_i \cdot P_i$ . Measuring the thermal power of the sample and knowing its specific power, the mass of radioactive material inside an assay is calculated according to Equation (1). Alternatively, one can determine the mass  $m_i$  of the  $i$ -th isotope composing the active material:

$$m_i = R_i \frac{W_{\text{item}}}{P_{\text{eff}}} = R_i \frac{W_{\text{item}}}{\sum_i R_i \cdot P_i}. \quad (2)$$

#### 5.1.2 Principle of operation

The LVC CHANCE calorimeter operates in the heat-flow-measurement mode. The sample inserted inside the measurement chamber generates heat as a consequence of its radioactivity. The reference block is kept at a constant-stable temperature and sensing Peltier elements convert the heat fluxes across different parts of the calorimeter into voltage signals  $V_i$  (either measuring or reference). Because the signal related to the heat flux is weak and subjected to various sources of noise (discussed further in this report), a *differential* measurement is implemented to significantly cancel out noise. In addition to the measurement cell, *ghost cells* are arranged in symmetrical configurations inside the calorimeter and act as reference cells (Figure 8). Simultaneous measurements of sample and reference voltages permit a differential cancellation of noise and offsets. As the calorimeter consists of two shells and the base, each of these parts contains its own measurement system and the output of the calorimeter at a given time is the sum of all three signals:

$$V_s = \sum_{l,c,r} (V_i^{\text{meas}} - V_i^{\text{ref}}) \quad (3)$$

where  $l$ ,  $c$  and  $r$  stand for the left, centre and right parts of the calorimeter. Where  $V_i^{\text{meas}}$  and  $V_i^{\text{ref}}$  are respectively signals registered by measuring sensors and reference sensors.



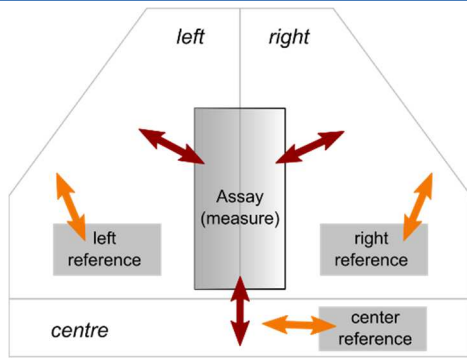


*Figure 8 - Thermal transfers between the nuclear assay and the left, right and centre parts of the calorimeter (not to scale). Each arrow depicts heat fluxes inside the calorimeter. These fluxes generate independent voltage signals  $V_i$  measured by an assembly of Peltier elements. All these contributions are summed according to Eq. (3) to give the signal voltage  $V_s$*

In order to precisely evaluate the heat flux generated by an assay, a “zero-signal”  $V_{BL}$  (baseline) of the calorimeter has to be recorded prior to measurements of active samples. Therefore, a preliminary measurement with the empty measurement chamber is performed, and the heat flux signal acquired at this step is called baseline. Only then, the main measurement can be done. After the measurement, the new baseline is recorded one more time to determine the average baseline  $\bar{V}_{BL}$ . The quantity of interest – the voltage drop originating from heat generated by an assay - is calculated as the difference between the signal with loaded sample and the average baseline:

$$\Delta V_{net} = V_s - \bar{V}_{BL} . \tag{4.1}$$

$$\bar{V}_{BL} = \frac{V_{BL1} + V_{BL2}}{2} . \tag{4.2}$$

$\Delta V_{net}$  only provides a qualitative probe of the heat generated by an active assay. Measurements of heat fluxes from Peltier elements thus requires prior knowledge of the sensitivity of these sensors, so that the total heat generated by the sample  $W_{item}$  is:

$$W_{item} = \frac{\Delta V_{net}}{S} , \tag{5}$$

where  $S$  ( $\mu V/mW$ ) is the sensitivity of the calorimeter. In order to obtain a quantitative probe, the calibration of  $S$  is mandatory. This calibration procedure is performed employing special cells able to provide a controllable power. The so-called “Joule effect cells” (EJ cells) are containers with embedded resistor. The electrical power dissipated in these resistors is fully converted to heat, hence enabling precise knowledge of the power generated by the assay. As for the measurements described in this section, a baseline is acquired, after which step power is injected into the EJ cell and  $\Delta V_{net}$  can be extracted. The calibration is explained in more details in Section 5.2.3.

## 5.2 Sources of uncertainties

In the following sections we start from the central quantity, the power dissipated by an assay, and “dissect” this quantity to find factors or causes that can influence the quality and precisions of its measurement. We denote the uncertainty/error associated to a quantity  $x$  by  $u(x)$ , the statistical average on a quantity  $z$  by an overhead bar ( $\bar{z}$ ) and its standard deviation by  $\sigma_z$ . Error-propagation rules are recalled in Appendix A, whereas details of the thermal design of the LVC CHANCE are explained in Appendix B.

### 5.2.1 Heat power

The power of an assayed item  $W_{item}$  (usually given in mW) can be retrieved from the differential heatflow of a calorimetric measurement in Equation (5). From Equations (5) and (A.1), the uncertainty on the measured power of the item  $W_{item}$  is:

$$u(W_{item}) = \frac{1}{S} \cdot u(\Delta V_{net}) + \frac{\Delta V_{net}}{S^2} \cdot u(S) . \tag{6}$$

These two main contributions  $u(\Delta V_{net})$  and  $u(S)$  to the uncertainty on  $W_{item}$  are assessed separately in the next sections.

### 5.2.2 Uncertainties on the heat flow

In this part we explore the origin of uncertainties on the “heat flow”  $\Delta V_{net}$ , the quantity measured by the calorimeter that is proportional to the heat dissipated by an assay. Errors on  $\Delta V_{net}$  directly affect performance of the calorimeter, therefore their causes must be well understood in order to prevent or minimize them. Here, we focus on experimental acquisition of the heat flow, with a statistical treatment of errors. Experiments showed that standard deviation of the out coming signal has significantly greater value compared to the resolution of the measuring devices. Therefore, it is assumed that the total uncertainty of each stabilized<sup>1</sup>-voltage (heat flow) signal  $V_j$  comes mainly from the standard deviation of the signal (it can be the baseline, or the signal when an assay is loaded):

$$u(V_j) \approx \sigma_j , \tag{7}$$

where the deviations on  $V_i$  stem from fluctuations of the regulation. High-frequency noise on voltage measurements due to the electronics of acquisition is contained in these fluctuations and is negligible compared to the low-frequency fluctuations of  $V_j$ . On the other hand, the noise of the regulation loop mainly impacts  $\sigma_j$  but its influence is not straightforward to characterise because of non-linearities in the feedback loop.

Following the propagation rule for statistical errors in Appendix A (Equation (A.2)), the standard deviation of the voltage  $V_s$  in Equation (3) is:

$$\sigma_s^2 = \sum_{l,c,r} \left( \sigma_{V_l}^2_{meas} + \sigma_{V_l}^2_{ref} \right) , \tag{8}$$

where  $l, c$  and  $r$  stand for the left, centre and right parts of the calorimeter. We obtain  $\sigma_s$  by measuring the standard deviation of the signals over a time lapse of signal stability. Practically, the acquisition software (Calisto) records the voltage signal  $V_s$  on a time chart, after all offsets have been cancelled, as shown on Figure 9. Thus, when it reaches stable values (without the sample it is called “baselines” ( $V_{BL1}$  and  $V_{BL2}$ ), and after its insertion, it is called “ $V_s$ ”) its average value  $\bar{V}_s$  and standard deviation  $\sigma_s$  can directly be measured, without explicit calculation of the left-hand term of Equation (8).

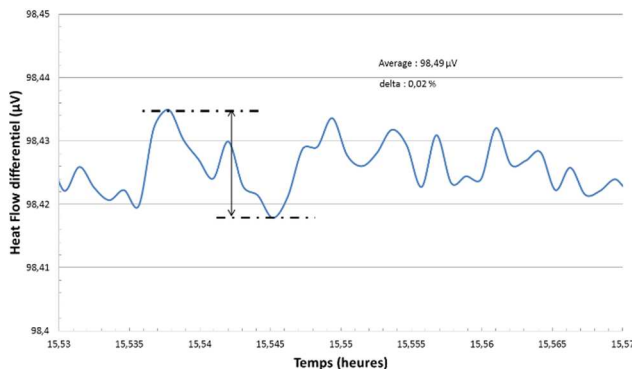


*Figure 9 - Example of a differential voltage signal ( $V_s(t)$ ) subjected to fluctuations around its average value of  $\bar{V}_s = 98.49 \mu V$  over time. The standard deviation for  $N$  samples is  $\sigma_s = \frac{1}{N} \sum_j (V_s(t_j) - \bar{V}_s)^2$*

<sup>1</sup> All voltage signals here are considered stable over time, so that they can be represented by their average value and standard deviation around it.



For Equation (3), the level of the baseline depends on two measurements, one before loading and one after unloading the specimen. Evaluation of the related uncertainty requires a more careful analysis. First, there could be a significant shift between  $V_{BL1}$  and  $V_{BL2}$ , so that there is an uncertainty of  $\pm|V_{BL1} - V_{BL2}|$ .<sup>2</sup> To this one has to add the statistical errors on each signal  $V_{BL1}$  and  $V_{BL2}$ :

$$u^2(\bar{V}_{BL}) = (V_{BL1} - V_{BL2})^2 + \sigma_{BL1}^2 + \sigma_{BL2}^2 . \tag{9}$$

This completes the evaluation of uncertainties on the heat flow. Therefore, the final uncertainty of  $\Delta V_{net}$  is:

$$u(\Delta V_{net}) = \sqrt{u^2(V_{meas}) + u^2(\bar{V}_{BL})} = \sqrt{\sigma_{BL1}^2 + \sigma_{meas}^2 + \sigma_{BL2}^2 + (V_{BL1} - V_{BL2})^2} . \tag{10}$$

In experiments, the standard deviations on the heat flow signal only weakly depends on the presence or absence of a sample inside the calorimeter, so that  $\sigma_{BL1}^2 \approx \sigma_{meas}^2 \approx \sigma_{BL2}^2 := 6\sigma_0^2$ , so that:

$$u(\Delta V_{net}) = \sqrt{18\sigma_0^2 + (V_{BL1} - V_{BL2})^2} . \tag{11}$$

$\sigma_0$  is the standard deviation on a Peltier signal, a quantity that, in principle, should be approximately equal for all segments of the calorimeter. One can observe in this last formula that there are two main factors influencing the accuracy of a measurement. First, fluctuations of the Peltier-voltage signals in  $\sigma_0$  depend on both regulation electronics and robustness of the thermal conception of the calorimeter. The second term, on the other hand, only depend on the thermal conception and accounts for the repeatability of measurements and thermal stability of the calorimeter. In cases where the calorimeter is very stable, such as  $(V_{BL1} - V_{BL2})^2 < \sigma_0^2$ , the uncertainty on the heatflow only depends on fluctuations of the Peltier voltages, in which case  $u(\Delta V_{net}) = 3\sqrt{2}\sigma_0$ .

### 5.2.3 Uncertainties on the sensitivity $S$

The sensitivity  $S$  of a calorimeter is determined ahead of measurements by a calibration procedure. A cell containing heating elements can deliver a controlled amount of heat current, equal to the power dissipated in the elements by Joule heating. Such a cell is loaded into the calorimeter and, after thermal stabilisation of it, pulses of constant power  $P_{in}$  are repeatedly (3x) input, with long enough periods between the pulses for stabilisation of the baseline. A scheme of the calibration procedure for  $P_{in} = 50mW$  is presented in the picture below:

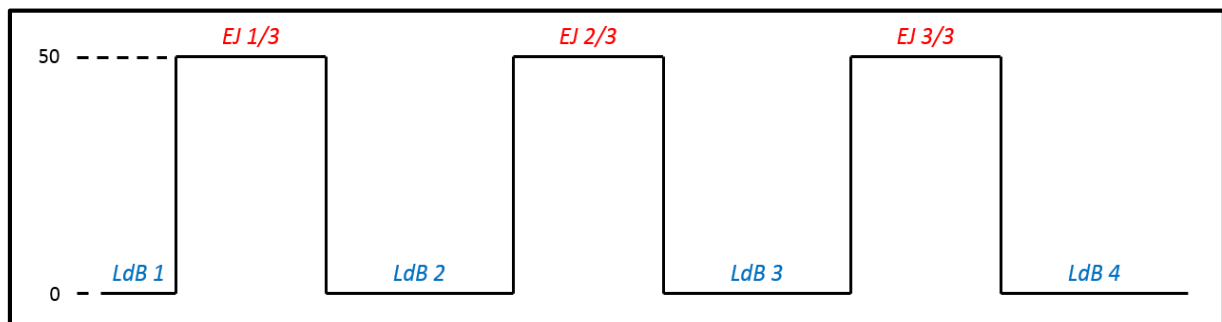


Figure 10 - Scheme of calibration procedure for 50mW Joule Effect.

Typically, the cell is heated for 24 hours and chilled for 36 hours, after which cycle it is heated again for 24 hours and so on. Next, the value of the power is changed and the procedure repeated for different power. It is very important to characterise the systematic error on  $S$  accurately, because it greatly

<sup>2</sup> This is the standard deviation on  $\bar{V}_{BL}$ , due to the statistics on only two values.

contributes to the total error on the measured power dissipated by an assay, affecting the performance specifications of the calorimeter.

The sensitivity is calculated as:

$$S = \frac{\Delta V}{P_{in}}, \tag{12}$$

where  $\Delta V$  is the net heatflow, measured in the same manner as  $\Delta V_{net}$ .

### 5.2.3.1 Uncertainty on a single Joule effect

First, the uncertainty on each Joule Effect measurement<sup>3</sup> can be calculated. Using rule (A.1) and equation (12), the uncertainty of the sensitivity is, for one set of datapoints  $i$ :

$$u(S_i) = \frac{u(\Delta V_i)}{P_{in,i}} + \frac{\Delta V_i \cdot u(P_{in,i})}{P_{in,i}^2}, \tag{13}$$

where  $P_{in,i}$  is the power of an item used for calibration.  $u(P_{in,i}) \approx \sigma_{P_{in,i}}$  is the standard deviation of the average value  $P_{in,i}$  over a duty cycle. This method yields as many uncertainties as available measurement points, and therefore is not the most meaningful way of obtaining accurate bounds for the sensitivity.

A second approach would be to undergo a simple statistical analysis. As a Joule effect is measured three times at  $p$  different power levels, the sensitivity coefficient can be averaged:  $\bar{S} = \frac{1}{3p} \sum_{i=1}^{3p} S_i$ , and its uncertainty given by the standard deviation  $\sigma_S$ . Unfortunately, this method is not refined enough because it could overestimate the error at high power and underestimate it at low powers. Indeed, we show that the error on  $S$  decreases with increased power. One can reasonably assume that  $u(\Delta V_i) \approx u(\Delta V) \approx \sigma_S$  and  $u(P_{in,i}) \approx u(P_{in})$ , because the noise on these quantities does not depend on their intensity. Moreover,  $S$  should be a constant. Substituting  $P_{in,i}$  by  $\frac{\Delta V}{S}$  in Eq. (13), one obtains the following relation:

$$u(S) = S \cdot [u(\Delta V) + u(P_{in})] \cdot \frac{1}{\Delta V}, \tag{14}$$

in other words, the error on  $S$  inversely scales with the heatflow.

A more careful estimation of  $u(S)$  can be obtained by considering more refined statistical analysis and fitting procedures, which are the subjects of next section.

### 5.2.3.2 Statistical analysis of the calibration

In order to determine  $S$  from a set of measurements  $\{P_{in,j} \pm u(P_{in,j}); \Delta V_j \pm u(\Delta V_j)\}$ , one can fit these data, weighted by their respective uncertainties. First, it is physically sound to consider that the sensitivity is constant, or in other words, that  $\Delta V$  is proportional to  $P_{in}$ . Following this assumption, the data points can be fitted linearly:

$$\Delta V = a \cdot P_{in} + b. \tag{15}$$

The fitting parameters  $a$  and  $b$  account for the sensitivity  $S$  and any offset in the heat flow ( $HF_0$ ), respectively. Among many methods of fitting the linear function in order to determine sensitivity, one can use the simple least squares method or the total least square method (TLS). However, because the measuring points are characterized by uncertainties that increase for lower powers, it seems reasonable to use a fitting method which uses weights based on these uncertainties. The methods used are described in the section 3.2.

<sup>3</sup> By a measurement we mean one pulse of heat and the baseline before and after it.



## 5.2.4 Uncertainties on derived quantities

Finally, having assessed the uncertainties on the measurement of the heat generated by an item, one can propagate this uncertainty to other derived quantities.

### 5.2.4.1 Total mass of active isotopes

From Equation (1) of the mass of active isotopes in the assay, using the propagation rule (Eq. (A.1)) the uncertainty on the mass yields:

$$u(m_{\text{item}}) = \frac{1}{P_{\text{eff}}} \cdot u(W_{\text{item}}) + \frac{W_{\text{item}}}{P_{\text{eff}}^2} \cdot u(P_{\text{eff}}). \quad (16)$$

### 5.2.4.2 Effective power and mass of active isotopes

The uncertainty on the specific power of an item  $P_{\text{eff}}$  can be retrieved from Eq. (2) employing Eq. (A.2):

$$u(P_{\text{eff}}) = \sqrt{\sum_i (R_i \cdot u(P_i))^2 + \sum_i (P_i \cdot u(R_i))^2}. \quad (17)$$

The sum of squared weighted errors is handful in this case, because the independence of the  $R_i$  with respect to  $P_i$ .

Similarly, the uncertainty associated to the mass of the  $i$ -th isotope  $m_i$  in Eq. (2) yields:

$$u(m_i) = \sqrt{(R_i \cdot u(m_{\text{item}}))^2 + (m_{\text{item}} \cdot u(R_i))^2}. \quad (18)$$

## 5.3 Analysis of experimental data

### 5.3.1 Calibration of the LVC CHANCE

For calorimeter calibration, Joule Effect (JE) cells were placed inside the measuring chamber and powers from 1 mW to 3000 mW were supplied to them. The calorimeter response (in  $\mu\text{V}$ ) was measured for each of these powers. For each case, the signal was also measured before placing the heat source (1st baseline) and after (2nd baseline) to determine the average zero response of the calorimeter.

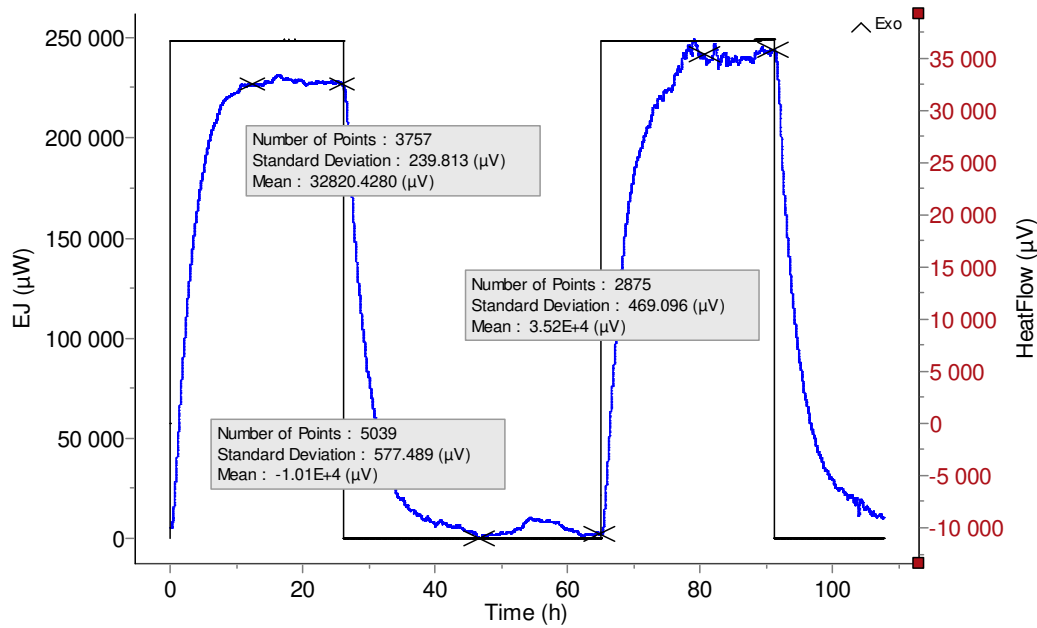


Figure 11 - Time chart of the heat flow recorded by Calisto (software) during two duty cycles of a “Joule-Effect” measurement at 250 mW of injected power. The blue line is the heat flow signal (right axis) and the black line is the Joule power (left axis).

In order to perform the measurement, after signal stabilization, the average value and standard deviation of heat flow were determined. Figure 3 shows how to perform the measurement for 250mW. The table below shows a summary of performed measurements:

Table 2- results of performed measurements. Values and uncertainties were calculated using formulas from chapter 5.

Power set point	Real injected power	u(IP)	Baseline before	u(Bb)	Baseline after	u(Ba)
mW	mW	mW	μV	μV	μV	μV
50	49,81	0,01	-8468,00	455,00	-11721,00	188,00
50	49,81	0,01	-5220,00	343,00	-7956,00	525,00
50	49,80	0,01	-7956,00	525,00	-8220,00	321,00
250	248,93	0,02	-10200,00	342,00	-10100,00	577,00
250	248,90	0,02	-10100,00	577,00	-10100,00	577,00
250	249,00	0,02	3964,00	451,00	3185,00	306,00
1000	998,50	0,01	-9669,04	320,87	-8605,27	336,76
1000	998,86	0,05	74,59	455,00	-5301,00	759,00

In order to calibrate the calorimeter, sensitivity had to be calculated. The statistical analysis of our dataset can be tackled in different ways. Both the absolute value and accuracy of the sensitivity will depend on the choice of this analysis. From the many available options we compare four of them. For the first analysis we calculate simple mean and weighted mean of the sensitivity obtained from each measurement. Then, we perform a “simple” (understand unweighted) linear regression and weighted regression as well. Finally, a total-least square regression is considered, not only taking into account the bias in the y direction, but also the bias in the x direction (error on the JE power). Procedure of sensitivity determination is described in detail in the next section.



### 5.3.2 Determination of sensitivity

After completing the calibration measurements, ie. consecutive JE and the corresponding response of the calorimeter, it was necessary to determine the sensitivity of the calorimeter ( $\mu\text{V}/\text{mW}$ ). Sensitivity, according to equation (7), is a parameter that allows to convert the output signal ( $\mu\text{V}$ ) into the thermal power of the sample ( $\text{mW}$ ). Because for low heat powers uncertainties of the measurements were greater than for measurements at higher powers, it was decided to use several methods determining sensitivity, compare them and choose the best way to convert the signal into the heat power of the sample.

#### 5.3.2.1 Mean

The JEs and corresponding heat flows were measured for each calibration point, i.e. for 50mw, 250mW and 1000mW. Therefore, the sensitivity can be calculated for each of them and the average of the obtained values can be calculated:

$$\bar{S} = \frac{1}{N} \sum_i S_i . \tag{19}$$

Using principle (A.1), sensitivity uncertainty will then be given as:

$$\bar{S} = \frac{1}{N} \sqrt{\sum_i u^2(S_i)} . \tag{20}$$

Sensitivity and its uncertainty were calculated using formulas (12) and (14):

*Table 3 - sensitivity calculated for each calibration point.*

Real injected power	u(IP)	HFnet	u(HFnet)	Sensitivity	u(S)
mW	mW	$\mu\text{V}$	$\mu\text{V}$	$\mu\text{V}/\text{mW}$	$\mu\text{V}/\text{mW}$
49,81	0,01	10404,50	3297,86	208,88	66,25
49,81	0,01	8255,00	2808,18	165,73	56,41
49,80	0,01	9110,00	813,51	182,93	16,37
248,93	0,02	42970,43	719,37	172,62	2,90
248,90	0,02	45300,00	941,18	182,00	3,80
249,00	0,02	46726,50	998,15	187,66	4,02
998,50	0,01	175637,16	1359,40	175,90	1,36
998,86	0,05	178676,21	5519,84	178,88	5,54

Using the above method, the value obtained was:

$$\bar{S} = \mathbf{182(32)} \mu\text{V}/\text{mW}$$

The obtained result is characterized by high measurement uncertainty (almost 18%). However, this result is disturbed by the high measurement uncertainty for 50mW power (~30% of uncertainty).

#### 5.3.2.2 Weighted mean

The measurements showed that for lower powers, the heat flow measurement is characterized by a greater relative measurement uncertainty. Therefore, contributions from these measurements should have less effect on the determination of sensitivity. For this purpose, mean sensitivity, calculated using weights based on heat flow uncertainties was defined as:



$$\bar{S}_w = \frac{\sum_i S_i \cdot w_i}{\sum_i w_i}, \tag{21}$$

where  $w_i = \frac{1}{u(\Delta V_i)}$ .

Using principle (A.1), sensitivity uncertainty will then be given as:

$$u(\bar{S}_w) = \frac{\sqrt{N}}{\sum_i w_i}. \tag{22}$$

Using the above method, the value obtained was:

$$\bar{S}_w = 178.4(1.5) \mu\text{V/mW}$$

### 5.3.2.3 Linear regression

Another way was to fit the linear function using the least squares method. This method was used in two variants: the first, matching the linear function  $y = ax + b$ , and the second, forcing  $b = 0$ . The results are presented below:

*Table 4 - linear regression, results.*

	a [uV/mW]	b [uV]
y=ax+b	176.8(1.4)	687(757)
y=ax	177.7(1.0)	-

In addition, the linear function  $y = ax + b$  was also fitted using the Total Least Squares (TLS) method. However, almost the same results as for the previous method were obtained. Table 4 and Figure 5 present linear fit using TLS method:

*Table 5 - TLS method, results.*

	a [uV/mW]	b [uV]
y=ax+b	176.9	661

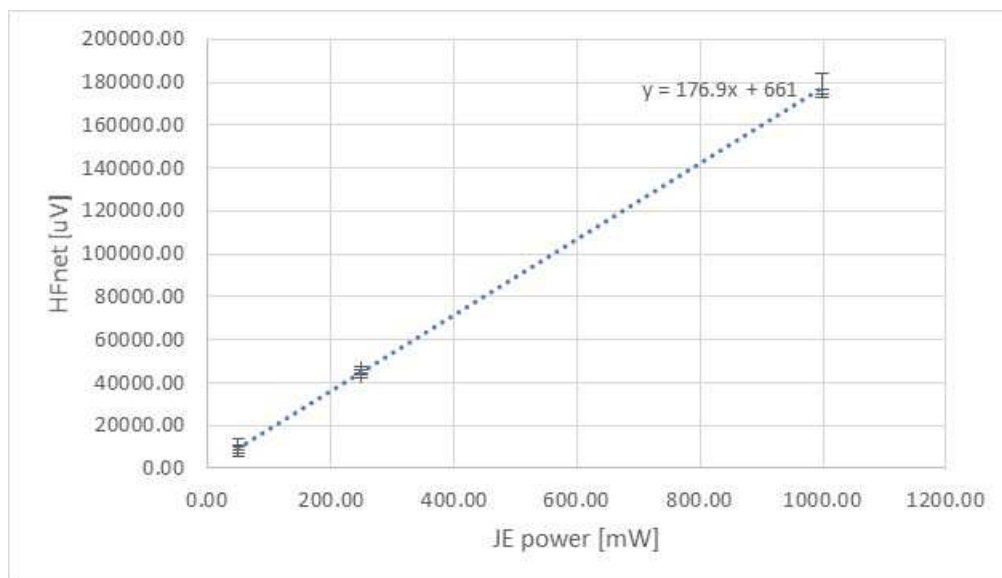


*Figure 12 - TLS fit method*

### 5.3.2.4 Weighted linear regression

As mentioned earlier, measurements for lower powers are characterized by greater measurement uncertainty. Thus, in the case of fitting a linear function, the impact of a given calibration point could be made dependent on its measurement uncertainty. In this way, using the Generalized Reduced Gradient algorithm (GRG), the following sum was minimized:

$$W = \sum_i \frac{(\widehat{\Delta V}_i - \Delta V_i)^2}{u(\Delta V_i)}, \tag{23}$$

where  $\widehat{\Delta V}_i$  is the value resulting from the fitting and  $\Delta V_i$  is the measured value. Similarly to the previous section, two variants of the function have been considered, i.e.  $y = ax + b$  and  $y = ax$ . The table below shows the results obtained:

Table 6 - Weighted linear regression, results.

	a [uV/mW]	b [uV]
y=ax+b	175.9	739
y=ax	177.2	-

The GRG algorithm has also been used to minimize the sum of the absolute value of the differences between the fitted value and the measured one  $|\widehat{\Delta V}_i - \Delta V_i|$ , giving similar results. The only difference was that for the function  $y = ax + b$ , regardless of the method (weighted or not),  $b$  converged to a value close to zero.

## 5.4 Summary

Using various methods, different values of sensitivity were obtained, ranging from 175.9 to around 182  $\mu\text{V/mW}$ . Depending on the method, the voltage cut-off was considered or not and it was 0  $\mu\text{V}$  or around 700 $\mu\text{V}$ . Table below shows the summarized results:

Table 7 - Summary of the results.

MEAN:		
weights	S [uV/mW]	
no	182(32)	
yes	178.4(1.5)	
LINEAR REGRESSION:		
weights	S [uV/mW]	HF <sub>0</sub> [uV]
yes	175.9	739
no	176.8(1.5)	687(757)
no	177.7(1.0)	-
yes	177.2	-
TLS	176.9	661

In order to determine the best method of converting heat flow into heat output, the average, relative fit error for each method was determined at each power  $P$ :

$$\Delta_P = \frac{1}{3} \sum_{i=1}^3 \frac{|\widehat{\Delta V}_i^P - \Delta V_i^P|}{\Delta V_i^P} \cdot 100\% . \tag{24}$$

The table and chart below present a summary of fit errors of the methods used:

Table 8 - Relative fit errors of considered methods, summary.

JE [mW]	mean	mean (weighted)	y=ax+b (TLS)	y=ax	y=ax+b	y=ax (weighted)	y=ax+b (weighted)
50,00	8,40%	9,07%	9,51%	9,21%	9,60%	9,32%	9,63%
250,00	2,84%	3,42%	3,23%	3,54%	3,22%	3,63%	3,33%
1000,00	2,51%	0,84%	0,84%	0,84%	0,84%	0,84%	0,84%

One can see that for the low power of the sample, regardless of the method, an error of around 10% occurs due to the calibration. The results show that the method of determining sensitivity has a significant impact on its value and potential measurement errors resulting from calibration. Therefore, depending on the range of operation of the calorimeter and planned powers of the samples according method of sensitivity determination should be used. For the dataset used, the regular mean is characterized by the flattest error distribution, i.e. for low powers the error is around 8.40% and it is smallest but for higher powers it is around 2.51% and it is grater compared to the other methods. Other methods, on the other hand, have a tendency to increase slightly the relative error for lower powers, but also decrease noticeably the error for higher powers.

On the other hand, the uncertainty-weighted mean method increases slightly the error for lower powers (9.07%), however, for higher powers decreases the error noticeably (from 2.51% to 0.84%). It is also worth recalling that a regular mean was characterized by the highest relative uncertainty (~18%), caused by less accurate measurements for lower powers, whereas for the other methods it was below 1%. Therefore, it is recommended to use uncertainty-weighted methods while determining the sensitivity.



Figure 13 - relative fit errors of considered methods, summary.

For the data used, the most efficient seems to use sensitivity based on the weighted mean or fitting function  $y = ax$  (using least squares method). Due to the simplicity, it seems most reasonable to use weighted mean. Therefore:

Sensitivity of CHANCE LVC:  $S = 178.4(1.5) \mu\text{V/mW}$



## 5.5 Conclusions

Calorimetry is a promising measurement method for determining the mass of radioactive content. Measurement of heat emission can potentially detect the entire content of the sample due to the fact that all radiation is eventually deposited as heat and it is not to be missed by calorimetry. However, the measurements carried out indicate that proper calibration and the method of converting the voltage signal into the thermal power of the sample is a key element determining the correct and accurate operation of the device. Analysing the data obtained during calibration, it can be concluded that the largest source of measurement uncertainty is the thermal stability of the system (fluctuations in the calorimeter response) and baseline instability before and after the measurement. These effects are significant for low power samples because the standard deviation of the signal and the difference between baselines is independent of the thermal power of the sample. Therefore, the accuracy of the measurement of the radioactive material content depend on the thermal power and the relative error is greater the higher the power is. It is worth emphasizing that additional sources of uncertainty in determining the mass of radioactive nuclides are the uncertainties of calculating effective power, i.e. measuring the ratio of a given isotope and its specific power. However, calorimetry, among other non-destructive methods, can significantly support the nuclear inventory process by detecting deeply buried or shielded emissions undetectable by other methods. The technology and the large measuring chamber that is used in CHANCE-LVC enables us to perform measurements for big waste drums regularly used in nuclear waste management.



## Appendix A – Error-propagation rules

Let  $x_1, x_2, \dots, x_n$  be measurable or observable quantities, with the (absolute) uncertainties  $u(x_i)$  associated to them. There often is a need to estimate the uncertainty on a quantity that is calculated from the  $\{x_i\}$ . Let  $y$  be this quantity and  $y = f(\{x_i\})$ , with  $f$  a function of the  $\{x_i\}$ . A Taylor expansion can be used to find small deviations around  $y$ :

$$y + u(y) \simeq f(\{x_i\}) + \sum_i \frac{\partial f}{\partial x_i} u(x_i) , \quad (\text{A.1})$$

if the parameters  $x_i$  are uncorrelated. Hence, the uncertainty  $u(y)$  is the sum of the uncertainties  $u(x_i)$ , weighted by partial derivative of  $f$  with respect to  $x_i$ . Moreover, if the parameters  $x_i$  are independent and their errors stem from statistical analysis, Equation (A.1) overestimates the error and a more favourable formula can be employed:

$$u(y) = \sqrt{\sum_i \left( \frac{\partial f}{\partial x_i} u(x_i) \right)^2} . \quad (\text{A.2})$$



## Appendix B – Thermal conception of the calorimeter

The calorimeter consists of a stack of layers. The alternating layers are made of alveolar foam (insulation layer) and aluminium (homogenizing layer). These layers are designed to thermally isolate the interior of the calorimeter from the influence of changes in ambient temperature (Figure 14)

Because the calorimeter's operating principle is based on a differential measurement of heat flow, inside the calorimeter there is a reference layer kept at a constant temperature (3<sup>rd</sup> controlled temperature in Figure 14). The block and measuring cells are the core of the calorimeter and the way in which these last elements are thermally insulated from the outside will be decisive for the performance of the calorimeter. Thus, the calorimeter must meet strict criteria for mitigating temperature variations and thermal flows. For this purpose, an additional layer kept at a constant temperature (2<sup>nd</sup> controlled temperature) is placed inside the calorimeter. In addition, the outermost layer is also kept at a constant temperature (1<sup>st</sup> controlled temperature). All this is done to best isolate the system from the environment, so that the heat flow measured by the system (Peltier elements) is disturbed as little as possible.

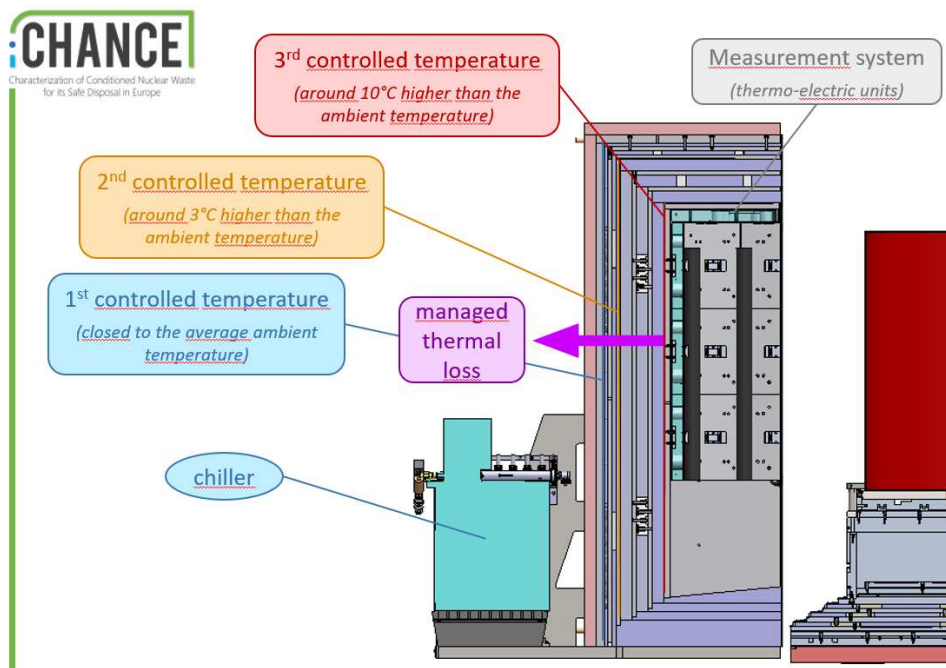


Figure 14 - principle of CHANCE calorimeter operation.

## 6 Bibliography

---

**ASTM** ASTM C1458-16, Standard Test Method for Non-destructive Assay of Plutonium, Tritium and <sup>24</sup>Am by Calorimetric Assay [Report]. - West Conshohocken, United States : ASTM International, 2016.

**Mason J.A.** The use of calorimetry for plutonium assay, A report submitted to the United Kingdom Atomic Energy Authority Safeguards R&D Project, [Report]. - 1982.

